Differential Use of the C-Type Lectins L-SIGN and DC-SIGN for Phlebovirus Endocytosis

Psylvia Léger[1†], Marilou Tetard[2,3†], Berthe Youness[1,2,4], Nicole Cordes[1], Ronan N. Rouxel[2,5], Marie Flamand[6] and Pierre-Yves Lozach[1,2*]

[1]CellNetworks − Cluster of Excellence and Department of Infectious Diseases, Virology, University Hospital Heidelberg, Heidelberg, Germany
[2]INRS-Institut Armand-Frappier, Laval, Canada
[3]Current address: Inserm UMR_S1134, Paris, France
[4]Reproduction Genetics Unit, Department of Gynecological Endocrinology and Reproductive Medicine, University Hospital, Heidelberg, Germany
[5]UR_0892 Unité de Virologie et Immunologie Moléculaire, INRA, CRJ, Jouy-en-Josas, France
[6]Structural Virology, Institut Pasteur, Paris, France
*Corresponding author: Pierre-Yves Lozach, e-mail: pierre-yves.lozach@med.uni-heidelberg.de

Abstract

Bunyaviruses represent a growing threat to humans and livestock globally. The receptors, cellular factors and endocytic pathways used by these emerging pathogens to infect cells remain largely unidentified and poorly characterized. DC-SIGN is a C-type lectin highly expressed on dermal dendritic cells that has been found to act as an authentic entry receptor for many phleboviruses (*Bunyaviridae*), including Rift Valley fever virus (RVFV), Toscana virus (TOSV) and Uukuniemi virus (UUKV). We found that these phleboviruses can exploit another C-type lectin, L-SIGN, for infection. L-SIGN shares 77% sequence homology with DC-SIGN and is expressed on liver sinusoidal endothelial cells. L-SIGN is required for UUKV binding but not for virus internalization. An endocytosis-defective mutant of L-SIGN was still able to mediate virus uptake and infection, indicating that L-SIGN acts as an attachment receptor for phleboviruses rather than an endocytic receptor. Our results point out a fundamental difference in the use of the C-type lectins L-SIGN and DC-SIGN by UUKV to enter cells, although both proteins are closely related in terms of molecular structure and biological function. This study sheds new light on the molecular mechanisms by which phleboviruses target the liver and also highlights the added complexity in virus−receptor interactions beyond attachment.

Keywords binding, bunyavirus, CD209, CD209L, C-type lectins, DC-SIGN, DC-SIGNR, endocytic motif, endocytosis, L-SIGN, phlebovirus, Rift Valley fever virus, uptake, Uukuniemi virus, virus receptor

Received 15 October 2015, revised and accepted for publication 8 March 2016, uncorrected manuscript published online 15 March 2016, published online 21 April 2016

The *Bunyaviridae* is a large family of RNA viruses, which comprises five genera (*Hantavirus*, *Nairovirus*, *Orthobunyavirus*, *Phlebovirus* and *Tospovirus*) (1). With over 350 isolates distributed worldwide, these viruses represent a global threat to livestock, agricultural productivity and human public health (1). Many cause serious diseases with high mortality rates in domestic animals and humans, such as fatal hepatitis, encephalitis and haemorrhagic fever. With the exception of hantaviruses, bunyaviruses are mainly spread by arthropods and consequently belong to the super group of arthropod-borne viruses (arboviruses) (1). Owing to their mode of transmission and an increasing number of outbreaks, bunyaviruses are considered emerging agents of disease. Currently, there are no vaccines or treatments approved for human use.

Bunyaviruses have a three-segmented negative-sense RNA genome that exclusively replicates in the cytosol. The viral

†These authors contributed equally to this work.

particles are enveloped and spherical with a diameter between 80 and 140 nm (1–3). The surface of particles is covered by two transmembrane glycoproteins, G_N and G_C, that are responsible for the attachment of the virus to target cells and for the subsequent acid-activated penetration from endosomal vacuoles (1,4,5). Inside the particles, the C-terminal tails of the virus glycoproteins are likely to interact with the ribonucleoproteins (RNPs) composed of the viral genome, the nucleoprotein N and the RNA-dependent RNA polymerase.

Transmission, tropism and cellular receptors remain largely uncharacterized (1). During natural transmission, bunyaviruses are introduced into the host skin through bites by infected arthropods. Dermal macrophages and dendritic cells (DCs), due to their location in the anatomical site of initial infection, are believed to play an important role in the bunyavirus spread throughout the host and infection (1). Both immune cell types are actively mobile upon stimulation and support infection by many bunyaviruses (6–12). In the late stages of infection, most host organs and tissues are invaded. The liver and hepatocytes appear as important targets of several bunyaviruses (13–16). Human liver sinusoidal endothelial cells (LSECs) express on their surface L-SIGN, a C-type (calcium-dependent) lectin specialized for the capture of foreign antigens (17).

L-SIGN, also known as CD209L or DC-SIGNR, is a type II membrane protein that binds high-mannose *N*-glycans through its C-terminal carbohydrate recognition domain (CRD) (18). It is present on the cell surface in different oligomerization states with tetramers having the highest avidity for a variety of substrates, including many viruses and viral glycoproteins (17,19). A direct role of L-SIGN in virus internalization beyond attachment has, however, not been demonstrated. L-SIGN shares 77% amino acid sequence homology with DC-SIGN, another human C-type lectin that has recently been shown to serve as an authentic entry receptor for many orthobunyaviruses and phleboviruses to infect dermal DCs (6,11,20).

It is apparent that bunyaviruses use other receptors than DC-SIGN. They can infect a large spectrum of tissues that do not express this lectin, e.g. LSECs and hepatocytes. To determine whether L-SIGN promotes phlebovirus

infection and whether this lectin can act as a receptor and explain the liver tropism of certain bunyaviruses, we analyzed virus binding, internalization and infection of various phleboviruses in L-SIGN-expressing cell systems. The results provide a comprehensive view of phlebovirus-L-SIGN interactions and establish a role of L-SIGN as a key host factor for viral attachment, and therefore, for infection.

Results

Rift Valley fever, Toscana and Uukuniemi viruses infect L-SIGN-expressing cells

Raji and HeLa cells stably expressing L-SIGN (Raji L-SIGN+ and HeLa L-SIGN+) were generated by transduction with a TRIPΔU3 lentiviral vector encoding human L-SIGN (Figure 1A) (21). To determine whether cells expressing L-SIGN support infection by bunyaviruses, we tested three phleboviruses, Rift Valley fever (RVFV), Toscana (TOSV) and Uukuniemi (UUKV) viruses. RVFV was rescued from plasmid DNAs and encoded the enhanced green fluorescent protein (EGFP) in place of the non-structural NSs protein (rRVFV-ΔNSs-EGFP) (22). The prototype lab strains of TOSV and UUKV were used. Cells were exposed to these viruses for 20 h and viral replication was assayed using flow cytometry either for EGFP in RVFV-infected cells or for newly synthetized viral proteins of TOSV and UUKV following immunostaining. To this latter end, a mouse ascitic fluid allowed detection of all the TOSV proteins whilst a monoclonal antibody (mAb) was used for detection of the UUKV protein N.

Raji and HeLa cells normally have low to no sensitivity to phlebovirus infection. As expected, parental Raji cells were nearly not infected with rRVFV-ΔNSs-EGFP, TOSV and UUKV at a multiplicity of infection (MOI) of 10 or less (Figure 1B). However, when L-SIGN was expressed, a significant fraction of cells was infected at an MOI of 1 (Figure 1B). The susceptibility of parental HeLa cells to infection by phleboviruses was minimal but significant at higher MOIs (Figure 1C). Nevertheless, infection of HeLa cells with RVFV-ΔNSs-EGFP, TOSV, and UUKV at various MOIs was dramatically increased when the lectin was expressed (Figure 1C). The capacity of L-SIGN to promote UUKV infection was confirmed using fluorescence
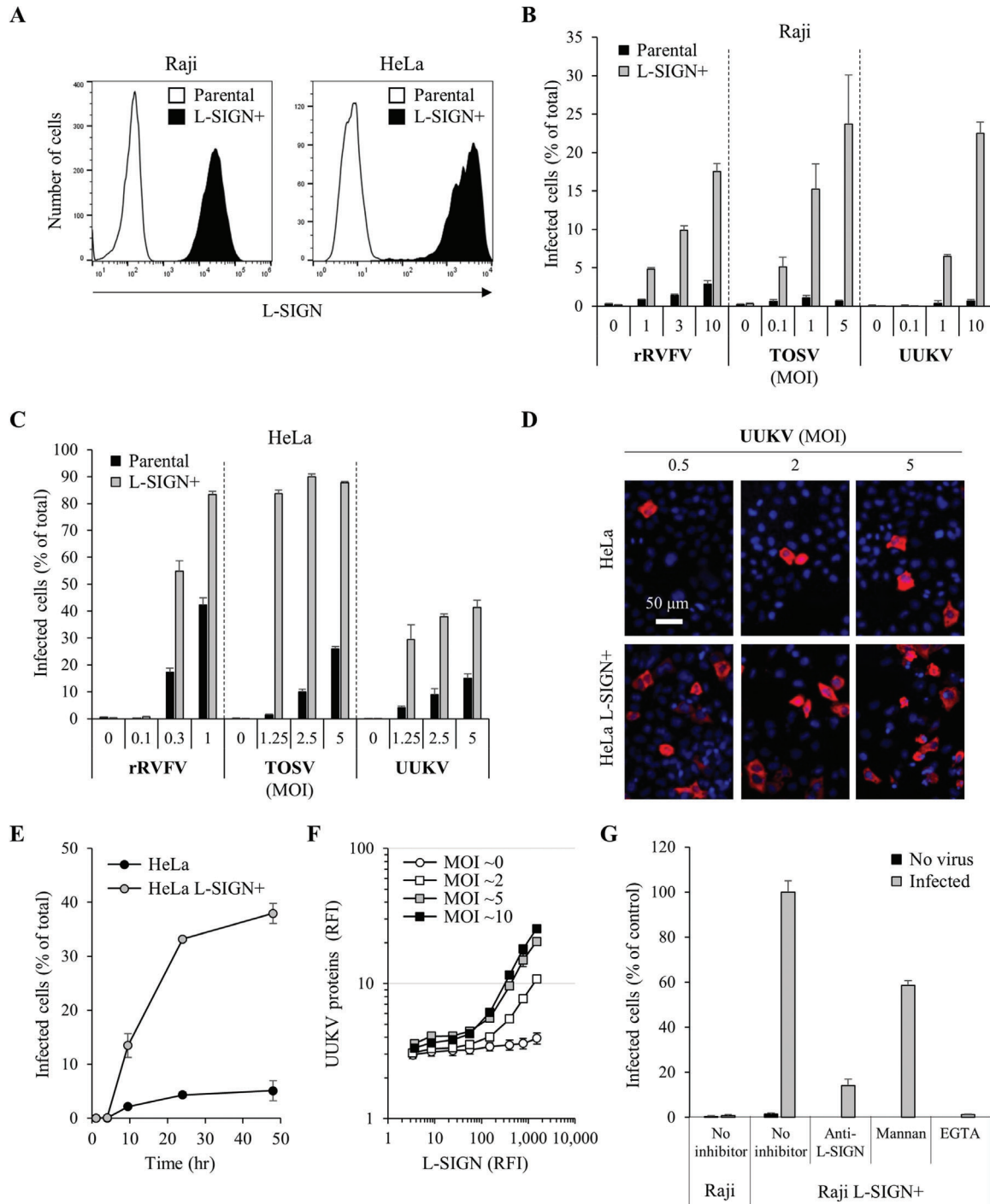
Figure 1: Legend on next page.

microscopy in HeLa cells (Figure 1D) and in HEK-293T cells (data not shown).

Together, these results showed that L-SIGN ectopically expressed in cell lines supports infection with different phleboviruses, and that UUKV could be used as a model to investigate the role of L-SIGN in bunyavirus entry. In all further experiments, we used UUKV because it is a validated BSL2 surrogate for arthropod-borne bunyaviruses of higher biosafety classification. Therefore, the use of UUKV allows approaches such as live cell imaging that is nearly impossible for pathogenic bunyaviruses, most of which must be handled in higher biosafety laboratories.

L-SIGN mediates infection

The fraction of L-SIGN-expressing HeLa cells infected with UUKV increased over time, emphasizing that progeny virus, and not input virus, was quantified in our flow cytometry-based assays (Figure 1E). Moreover, concomitant staining against L-SIGN and UUKV proteins showed that infection increased with increasing L-SIGN expression (Figure 1F). To confirm that the infection was mediated by

L-SIGN, we utilized inhibitors of the lectin such as EGTA, mannan, and the neutralizing mAb 1621. EGTA inhibits the L-SIGN binding function by extracting the bound calcium, and mannan is a competitor of insect-derived glycans (23). The increase in infectivity due to L-SIGN expression was significantly reduced in cells treated by these inhibitors (Figure 1G). Together, these results clearly indicate that UUKV infection is mediated by L-SIGN.

L-SIGN enhances binding of UUKV to cells

To examine whether L-SIGN enhanced infection by promoting phlebovirus binding, we utilized fluorescently labeled UUKV particles. These particles can be seen as single spots using confocal microscopy; no significant impact of labeling on infectivity is observed (5,6). Virus binding to L-SIGN-expressing HeLa cells was imaged using confocal microscopy (Figure 2A). The number of particles bound per HeLa cell was significantly increased in the presence of L-SIGN (Figure 2B).

Binding to L-SIGN-expressing Raji cells was also analyzed using flow cytometry. When Raji L-SIGN+ cells

Figure 1: L-SIGN mediates infection by RVFV, TOSV and UUKV. A) Raji and HeLa cells stably expressing L-SIGN were generated by transduction with a lentiviral vector encoding human L-SIGN. The expression of L-SIGN at the cell surface was detected using flow cytometry after immunostaining with the Fab 1621P, which recognizes the CRD of the lectin. B) Parental and L-SIGN-expressing Raji cells were infected with different multiplicities of infection (MOI) of rRVFV, TOSV, or UUKV for 20 h. The recombinant RVFV strain expressed EGFP in place of the virulent non-structural protein NSs (rRVFV-ΔNSs-EGFP). Infection was assessed using flow cytometry either for EGFP in RVFV-infected cells or for newly intracellular TOSV antigens and UUKV protein N following immunostaining with a mouse immune ascitic fluid and the mouse mAb 8B11A3, respectively, and an AF647-conjugated anti-mouse mAb. Results are shown as the percentage of EGFP-positive cells or the percentage of viral protein-positive cells (% of total). C) Infection by rRVFV, TOSV, or UUKV was performed, monitored and analyzed in parental and L-SIGN-expressing HeLa cells following the same procedure outlined in (B). D) Parental and L-SIGN-expressing HeLa cells were exposed to various MOIs of UUKV. The day after, infected cells were immunostained for the intracellular UUKV nucleoprotein N using the anti-N primary mAb 8B11A3 and an AF568-coupled anti-mouse secondary mAb (red). Nuclei were stained with Hoechst (blue) and samples analyzed using wide-field microscopy. E) UUKV infection (MOI ~1) was monitored over 48 h in parental and L-SIGN-expressing HeLa cells (HeLa L-SIGN+) using flow cytometry analysis, as described in (B). F) L-SIGN-expressing Raji cells were exposed to UUKV and harvested 8 h later. Concomitant immunostaining of infected cells allowed the detection of both L-SIGN (Fab 1621P) and newly synthetized UUKV intracellular proteins (pAb U2). Various subpopulations of cells were selected using flow cytometry for increasing expression of the lectin (*y*-axis), and each subpopulation was independently analyzed for infection (*x*-axis). UUKV proteins and L-SIGN expression are given as the relative fluorescence intensities (RFI) associated with the 10,000 cells analyzed using flow cytometry. G) L-SIGN-expressing Raji cells (Raji L-SIGN+) were infected with UUKV (MOI ~10) in the presence of inhibitors blocking L-SIGN, namely mannan (20 μg/mL), EGTA (5 mM), and the neutralizing mAb 1621 (anti-L-SIGN, 25 μg/mL). Intracellular viral antigens were detected by immunostaining with an anti-UUKV pAb followed by an incubation with AF647-conjugated secondary Ab. Infection was analyzed using flow cytometry 20 h later and normalized to infection of L-SIGN-expressing Raji cells in the absence of inhibitors (% of control).
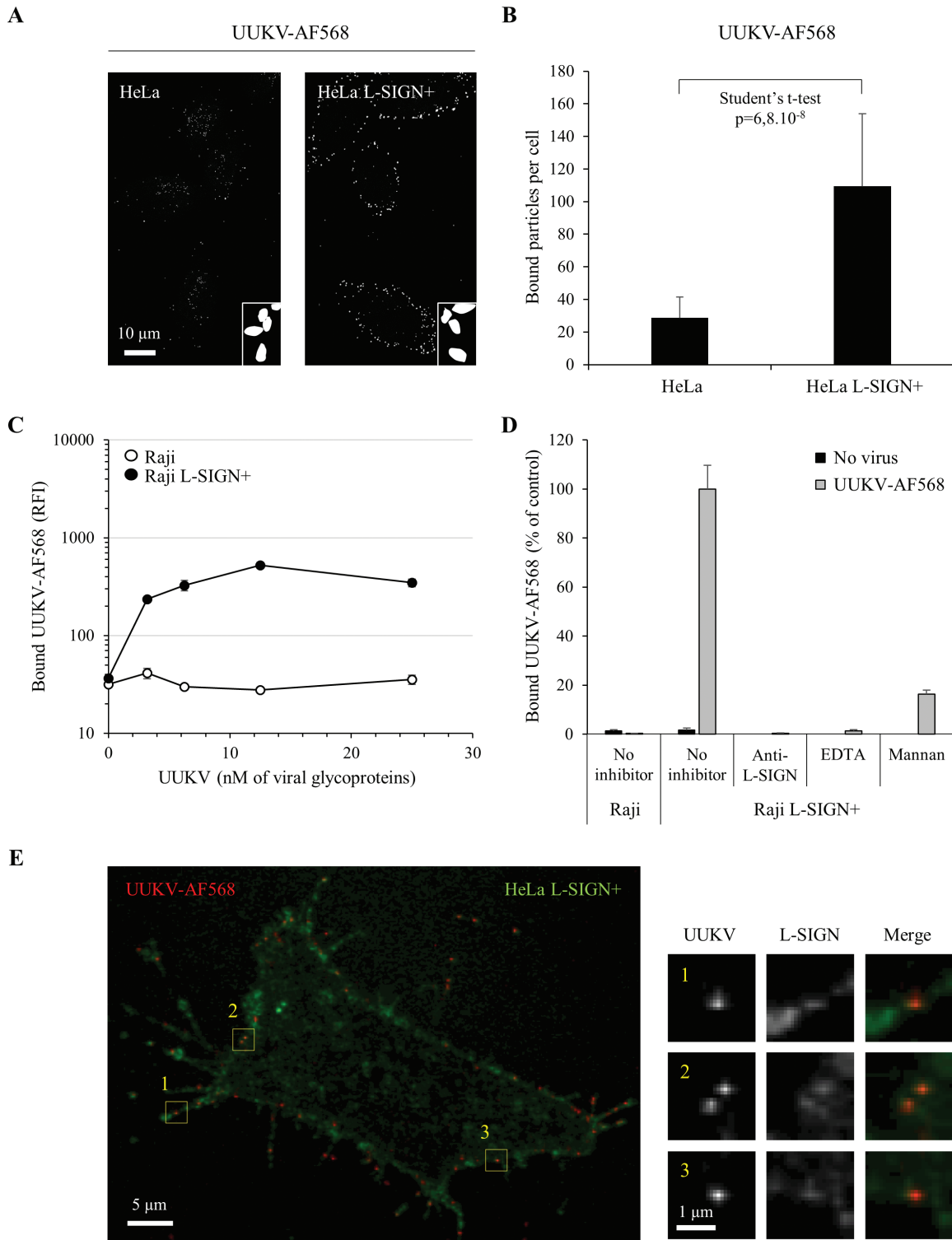
Figure 2: Legend on next page.

were exposed to various amounts of Alexa Fluor (AF) 568-conjugated UUKV (UUKV-AF568), improved binding correlated with an increasing concentration of input virus under conditions in which no binding was observed to parental cells (Figure 2C). The presence of L-SIGN inhibitors, namely the neutralizing mAb 1621, mannan and ethylenediaminetetraacetic acid (EDTA), which, like EGTA, blocks the lectin by extracting the bound calcium, impaired virus binding on Raji L-SIGN+ cells (Figure 2D). Confocal microscopy, following immunostaining with an anti-L-SIGN mAb that recognizes the CRD of the lectin showed that the bound UUKV-AF568 particles were associated with L-SIGN-containing spots and areas of different sizes (Figure 2E). These were most likely viruses bound to lectin molecules in a close vicinity of additional, non-engaged L-SIGN proteins (i.e. within lectin tetramers or clusters). Altogether, these experiments show that L-SIGN supports UUKV binding through specific and direct interactions.

UUKV is efficiently internalized into L-SIGN-expressing cells

To test whether L-SIGN facilitates UUKV endocytosis, we exposed HeLa L-SIGN+ cells to UUKV-AF568 at 4°C, washed them to remove unbound material, and rapidly warmed to 37°C to allow internalization. Cells were fixed and viral particles were then imaged using confocal microscopy. After warming (20 min) a significant fraction of particles were located in the cytosol (Figure 3A). Spinning-disc confocal video-microscopy of live cells also showed that UUKV-AF568 was taken up by HeLa cells expressing L-SIGN (Movie S1, Supporting Information).

We have recently showed that UUKV relies on endosomal acidification for infectious entry (4,5). We observed that UUKV infection of L-SIGN-expressing cells was also sensitive to agents that neutralize vacuolar pH, such as ammonium chloride (NH_4Cl), a lysomotropic weak base and bafilomycin A1, a vacuolar-type H + −ATPase inhibitor (Figure 3B,C). These demonstrate that UUKV entry into L-SIGN-expressing cells involves endocytic internalization and acidification.

L-SIGN relies on the LL motif in its cytosolic tail for endocytosis

The L-SIGN cytosolic tail carries several sequence motifs and amino acids that are believed to be involved in signaling, endocytic internalization and intracellular trafficking (24). These include serine, lysine and threonine residues, but also, an acidic cluster as well as a dileucine-based motif, LL (Figure 4A). The classical LL motif is also present in the cytosolic tail of the closely related C-type lectin DC-SIGN. When the LL motif is absent, DC-SIGN by itself is no longer able to promote UUKV internalization and infection (6). To investigate the importance of this motif in the L-SIGN-dependent UUKV infection, we generated an L-SIGN mutant devoid of the LL sequence (L-SIGN$_{LL}$) by site-directed mutagenesis (Figure 4A). HeLa cells were transduced with a TRIPΔU3 lentiviral vector encoding the wild-type (WT) form of L-SIGN or the endocytosis-defective mutant (L-SIGN$_{LL}$), and then sorted for populations expressing similar levels of the lectin molecules (HeLa L-SIGN low + and HeLa L-SIGN$_{LL}$+, Figure 4B). Both HeLa L-SIGN low + and HeLa L-SIGN$_{LL}$+ cell lines were used in all further

Figure 2: L-SIGN is responsible for UUKV binding to cells through direct interactions. A) UUKV-AF568 (MOI ∼ 1) was bound to L-SIGN-expressing HeLa cells on ice and imaged using confocal microscopy. Spots are cell-associated particles seen in a series of z stacks merged to one plane. Fields with many cells are shown and depicted on the bottom right of each picture. B) Bound particles per cell ($n = 20$) were counted in eight independent fields from (A). C) Serial dilutions of UUKV-AF568 were bound to Raji and Raji L-SIGN+ cells on ice for 2 h. UUKV-AF568 inputs were normalized according to the concentration of viral glycoproteins. Virus binding is expressed as the cell-associated RFI measured using flow cytometry. D) UUKV-AF568 was bound to Raji and Raji L-SIGN+ cells (10 nM of viral glycoproteins, corresponding to a MOI ∼0.5) on ice for 2 h in the presence of L-SIGN inhibitors, namely the neutralizing mAb 1621 (anti-L-SIGN, 25 μg/mL), mannan (20 μg/mL) and EDTA (5 mM). Binding was quantified using flow cytometry and normalized to binding to Raji L-SIGN+ cells in the absence of inhibitors (% of control). E) UUKV-AF568 was bound to L-SIGN-expressing HeLa cells (MOI ∼ 1) on ice for 2 h. After fixation and permeabilization, the lectin was detected using the anti-L-SIGN primary mAb 162 and an AF488-coupled secondary anti-mouse Ab. UUKV (red) and L-SIGN (green) were imaged using confocal microscopy and are shown in one focal plane. Magnifications of association between UUKV and L-SIGN (numbered yellow squares) are shown on the right.
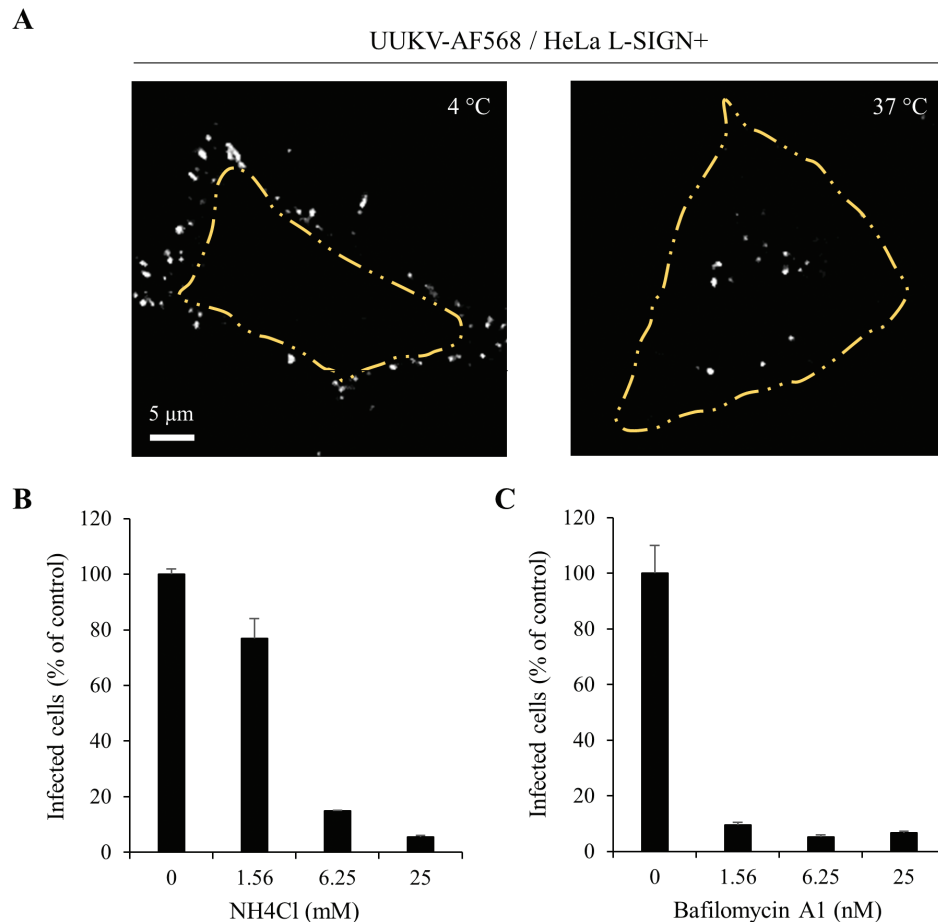
Figure 3: UUKV relies on endosomal acidification for L-SIGN-dependent infection. A) UUKV-AF568 was bound to L-SIGN-expressing HeLa cells (MOI ~1) on ice for 2 h. Infected cells were then washed and maintained in the cold or rapidly warmed to 37°C for 20 min to trigger viral entry. After fixation, viral particles were imaged using confocal microscopy. Spots are cell-associated virus particles seen in one focal plane. B and C) HeLa cells expressing L-SIGN were pre-treated with varying concentrations of drugs that neutralize the endosomal pH, namely NH_4Cl (B) and Bafilomycin A1 (C), and then exposed to UUKV (MOI ~10) in the presence of the perturbants. Infected cells were harvested 20 h later and immunostained for the UUKV nucleoprotein N as described in Figure 1B. Infection was analyzed using flow cytometry and normalized to L-SIGN-expressing Raji cells infected in the absence of inhibitor (% of control).

experiments aiming to assess the role of the LL endocytic motif of L-SIGN in UUKV entry and infection.

To assess the endocytosis of L-SIGN, cells were incubated with the anti-L-SIGN fragment antigen binding (Fab) 162 on ice, and rapidly warmed to 37°C to allow the internalization of the lectin. Warming induced a dramatic redistribution of the WT L-SIGN receptors within 10 min, consistent with an intracellular accumulation of the lectin, and in agreement with a previous study (Figure 4C) (25). In marked contrast, we found that the majority of the

mutant L-SIGN$_{LL}$ molecules remained at the cell surface after 30 min (Figure 4C). Together, our data indicate that the WT lectin receptor is efficiently internalized into HeLa cells upon mAb binding and that the LL motif is required for effective L-SIGN endocytosis.

UUKV does not depend on L-SIGN endocytosis for infection

We then assessed whether loss of the LL motif impaired UUKV infection. HeLa cells expressing similar levels of L-SIGN and L-SIGN$_{LL}$ molecules, i.e. HeLa L-SIGN
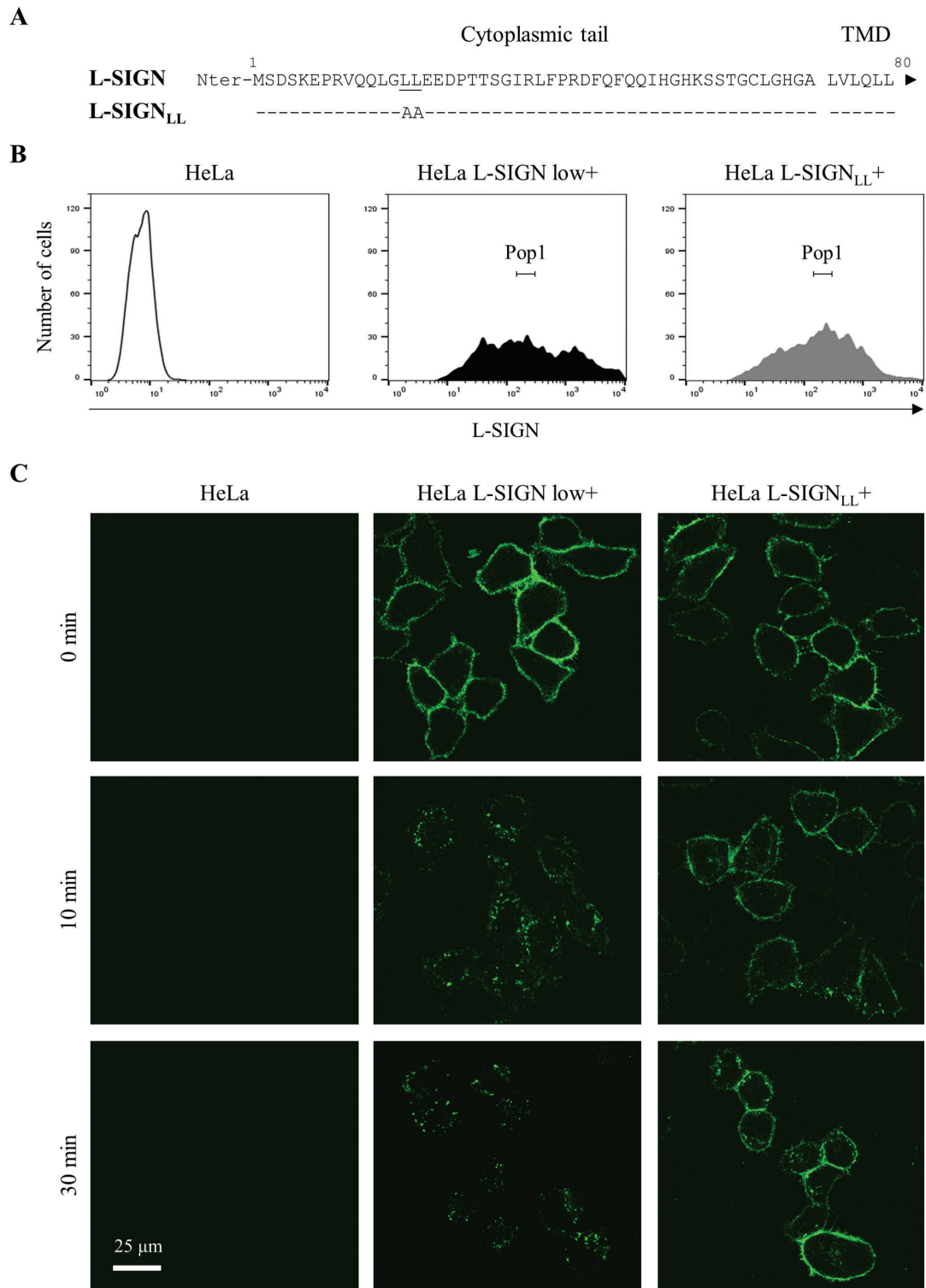
A

Cytoplasmic tail   TMD

L-SIGN   Nter-MSDSKEPRVQQLGLLEEDPTTSGIRLFPRDFQFQQIHGHKSSTGCLGHGA LVLQLL ▶

L-SIGN_LL   --------------AA----------------------------------- ------

B

C

Figure 4: Legend on next page.

low + and HeLa L-SIGN$_{LL}$+ (Figure 4B), were exposed to UUKV at various MOIs. We found that HeLa cells expressing L-SIGN$_{LL}$ were as efficiently infected as L-SIGN-expressing cells (Figure 5A). When infection was analyzed in cell populations selected for identical expression of the WT lectin and the endocytosis-defective mutant (Pop1, Figure 4B), similar results were observed (Figure 5B). These data suggest that L-SIGN endocytosis is dispensable for efficient UUKV infection.

To determine whether the endocytosis-defective form of L-SIGN internalizes the virus, L-SIGN$_{LL}$-expressing HeLa cells were exposed to UUKV-AF568 in the cold, washed to remove unbound particles and rapidly warmed to 37°C to allow endocytosis. After fixation and permeabilization, infected cells were immunostained with anti-L-SIGN mAb, and analyzed using confocal microscopy. We found that L-SIGN$_{LL}$ bound UUKV with the same efficiency as cells expressing the WT lectin (Figure 5C). After warming (30 min) several particles were seen internalized into both L-SIGN- and L-SIGN$_{LL}$-expressing cells (Figure 5D). At this time, viruses accumulated in the perinuclear region, a typical location for late endosomal (LE) vesicles. However, while most internalized particles remained associated with lectin-containing endosomal vacuoles in L-SIGN-expressing cells, viruses were mainly found in vesicles devoid of the lectin in cells expressing the endocytosis-defective mutant of L-SIGN. This supports the view that L-SIGN by itself does not promote UUKV internalization.

Role of DC-SIGN and L-SIGN in UUKV infection

The C-type lectin DC-SIGN is closely related to L-SIGN, but unlike L-SIGN, acts as a true endocytic receptor for UUKV (6). The LL-based motif in the DC-SIGN cytosolic tail is critical for both lectin endocytosis and UUKV entry (6). To further examine the role of DC-SIGN and L-SIGN in phlebovirus infection, we used Raji and HeLa cell lines expressing comparable levels of lectin molecules on their surface, as evidenced by immunostaining with the Fab 1621P that recognizes the CRD of both DC-SIGN and L-SIGN (Figure 6A,B). We found that Raji and HeLa cells expressing L-SIGN (Raji L-SIGN+ and HeLa L-SIGN+) were less efficiently infected by UUKV than DC-SIGN-expressing cells (Raji DC-SIGN+ and HeLa DC-SIGN+). Even higher differences were observed at lower MOIs (Figure 6C,D). However, the capacity of the two lectins to enhance UUKV infection was much closer in HeLa cells than in Raji cells (Figure 6C,D).

We then compared the importance of the LL-based motif in the cytosolic tail of L-SIGN and DC-SIGN for UUKV infection. HeLa cells expressing each lectin or their LL-based mutant form (Figures 4B and 7A) were exposed to UUKV at a MOI of 1 for 7 h, and infection was assessed using flow cytometry for the newly synthetized viral protein N. In contrast to the endocytosis-defective mutant of L-SIGN, the LL-based mutant of DC-SIGN was less efficient in promoting UUKV infection than the WT molecule (about a 50% decrease, Figure 7B). These results confirm that the major difference between DC-SIGN and L-SIGN regarding UUKV infectious entry is that L-SIGN rather serves as an attachment factor for the virus.

To compare the timing of the acid-requiring step after endocytic entry into DC-SIGN- and L-SIGN-expressing HeLa cells, we bound virus to cells on ice and rapidly shifted the temperature to 37°C to allow endocytosis. NH$_4$Cl was added at different times after warming to prevent further virus penetration. The entry process was

Figure 4: The cytoplasmic LL motif of L-SIGN is critical for the sorting of the lectin into the endocytic machinery.
A) Schematic representation of the mutation introduced into the L-SIGN cytoplasmic tail (LL/AA, L-SIGN$_{LL}$). The endocytic LL-based motif is underlined. TMD stands for transmembrane domain. B) HeLa cell lines expressing either the WT form (HeLa L-SIGN low+) or the LL-based mutant of L-SIGN (HeLa L-SIGN$_{LL}$+) were generated by retroviral transduction and sorting for similar expression of the lectin. The cell surface was then immunostained with the PE-conjugated anti-L-SIGN Fab 1621P and analyzed using flow cytometry. Cell populations that express comparable amounts of L-SIGN and L-SIGN$_{LL}$ at their surface (Pop1) were assessed for UUKV infection in Figure 5B. C) Subcellular localization of L-SIGN and L-SIGN$_{LL}$. HeLa L-SIGN low + and HeLa L-SIGN$_{LL}$+ cells were incubated with the anti-L-SIGN FITC-conjugated Fab 162F on ice for 1 h, washed to remove unbound Abs, and either maintained in the cold or rapidly warmed to 37°C for up to 30 min. After fixation, the cellular localization of the lectins was examined using confocal microscopy.
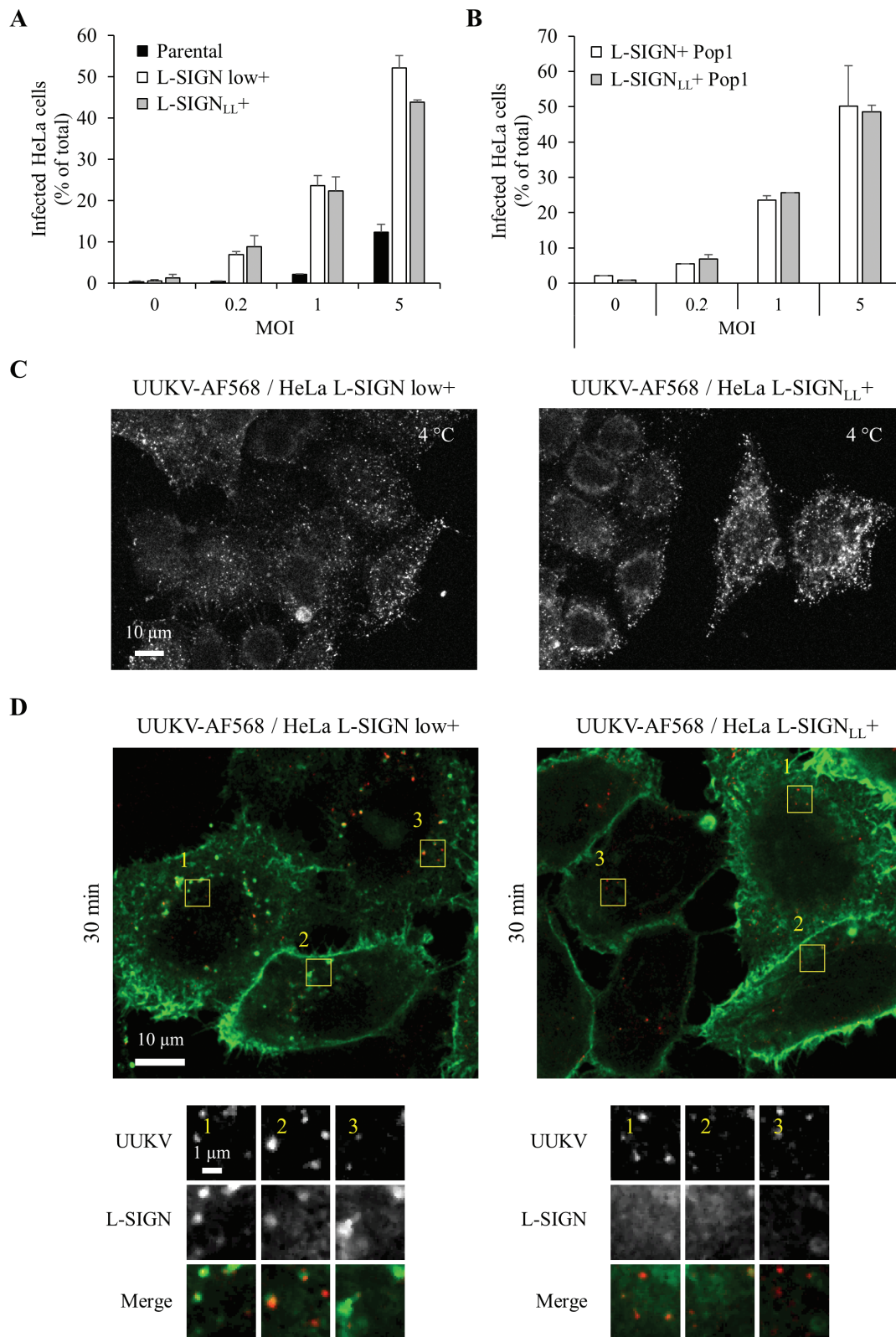
Figure 5: Legend on next page.

faster in cells expressing DC-SIGN (Figure 7C). Infectious penetration started after a 5-min lag and reached a maximum level after 20 min in HeLa DC-SIGN+ cells versus 80 min in HeLa L-SIGN+ cells (Figure 7C). Spinning-disc confocal live imaging showed that the overall dynamics of virus uptake and intracellular trafficking is faster in HeLa cells expressing DC-SIGN versus L-SIGN (Movies S1 and S2). Taken together these data indicate that the general properties and dynamics of UUKV infection are overall faster and more efficient in cells expressing DC-SIGN than L-SIGN.

Discussion

The expression of L-SIGN on LSECs and its capacity to bind *N*-glycans on viral glycoproteins make this lectin a candidate receptor responsible for liver tropism of enveloped hepatotropic viruses. As an immune receptor on endothelial cells, L-SIGN is thought to be critical for the capture, processing and subsequent presentation of foreign antigens, thus promoting the initiation of the acquired immune system. It has been proposed that some viruses (including arboviruses of the flavi- and alphavirus families) have found a way to use L-SIGN for attachment and to promote viral entry and infection (17,26).

In this study, we have expanded these observations to bunyaviruses. We found that several phleboviruses, namely RVFV, TOSV and UUKV, use L-SIGN to infect cells expressing the lectin ectopically. Others have recently shown that L-SIGN enhances infection by rhabdoviral particles pseudotyped with the glycoproteins of the phlebovirus severe fever with thrombocytopenia syndrome, but not with those of RVFV or the orthobunyavirus La Crosse (LACV) (11). The engagement of multiple viral glycoproteins by homo-tetrameric lectins is critical for high-avidity interactions between the closely related C-type lectin DC-SIGN and the arbovirus dengue virus from the *Flaviviridae* family (27). Rhabdoviruses and bunyaviruses differ significantly with regard to the assembly and maturation of viral progeny. While pseudotyped particles are unquestionably of interest to study many aspects of virus transmission and entry, the structural organization of *N*-glycans on their surface may not exactly reflect the organization on RVFV and LACV viral particles, which in turn, could favor less-efficient virus binding to C-type lectins and infection.

Although high-mannose *N*-glycans are typical for insect-derived glycoproteins, bunyaviruses are usually rich in high-mannose *N*-glycans even when produced in mammalian cells (6,28–30). This suggests that these viruses do not require production in insects to be recognized by L-SIGN. After introduction into the host dermis by infected arthropods and the initial infection, bunyaviruses conserve the ability to use C-type lectins with high affinity for mannose residues, such as L-SIGN, to target and infect new tissues in further rounds of infection. Although the interaction of additional bunyaviruses with L-SIGN must be assessed experimentally, it is likely that many can use L-SIGN as a receptor.

Figure 5: L-SIGN by itself is not required for UUKV internalization and infection. A) HeLa L-SIGN low + and HeLa L-SIGN$_{LL}$+ cells were exposed to UUKV at various MOIs. Infected cells were immunostained for the viral protein N, using the anti-N mAb 8B11A3, and analyzed using flow cytometry 7 h later. Infection is expressed as the percentage of N-positive cells (% of total). B) L-SIGN- and L-SIGN$_{LL}$-expressing HeLa cells were infected with varying MOIs of UUKV and harvested 7 h later. Samples were immunostained for newly synthetized UUKV proteins (anti-N mAb 8B11A3) and for the surface expression of the lectin (anti-L-SIGN Fab 1621P). Infection was quantified using flow cytometry in cell subpopulations selected for identical levels of lectin expression (L-SIGN low + Pop1 and L-SIGN$_{LL}$+ Pop1 in Figure 4B). C) Fluorescent UUKV particles (UUKV-AF568, MOI ∼1) were bound to HeLa cells expressing L-SIGN (HeLa L-SIGN low+) or its endocytosis-defective form (HeLa L-SIGN$_{LL}$+) on ice for 2 h before fixation and confocal imaging. Spots are cell-associated particles seen in a series of z stacks merged to one plane. D) UUKV-AF568 (MOI ∼1) was bound to HeLa cells expressing L-SIGN (HeLa L-SIGN+) or to the L-SIGN endocytosis-defective mutant (HeLa L-SIGN$_{LL}$+) at 4°C for 2 h. Cells were washed to eliminate unbound viruses and either maintained on ice or warmed for 30 min. Samples were imaged using confocal microscopy after fixation, permeabilization and staining of the lectin with the anti-L-SIGN primary mAb 162 followed by an incubation with an AF488-conjugated secondary Ab. Red spots are cell-associated virus particles seen in one focal plane. The lectin appears in green. Some magnifications (numbered yellow squares) are shown on the bottom.
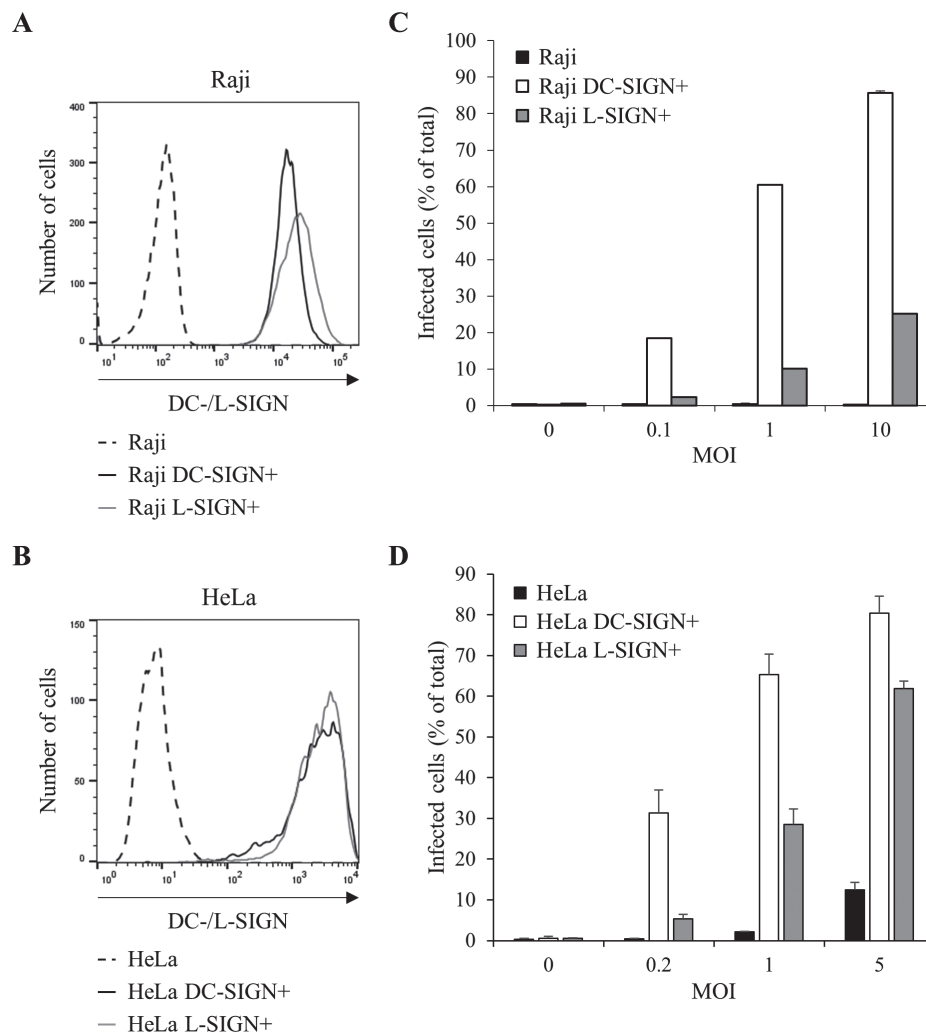
Figure 6: Efficiency of DC-SIGN and L-SIGN in mediating UUKV infection. Expression of either A) DC-SIGN or B) L-SIGN at the surface of Raji and HeLa cell lines (Raji DC-SIGN+, HeLa DC-SIGN+, Raji L-SIGN+ and HeLa L-SIGN+) was detected using flow cytometry after immunostaining with the Fab 1621P, which recognizes the CRD of both L-SIGN and DC-SIGN. C) DC-SIGN- and L-SIGN-expressing Raji cells were infected with UUKV at different MOIs and analyzed 20 h post-infection using flow cytometry after immunostaining against the UUKV nucleoprotein N. Infection is expressed as the percentage of N-positive cells (% of total). D) Infection of HeLa cell lines expressing either DC-SIGN or L-SIGN with UUKV was performed, monitored and analyzed following the same procedure as that (C).

One of the phleboviruses, UUKV, was used to further analyze the role of the lectin in the infection process. Most bound UUKV particles were seen to be associated with L-SIGN. DC-SIGN was reported to bind UUKV directly via interactions with high-mannose N-glycans on the glycoproteins G_N/G_C (6). When cells expressing L-SIGN were exposed to UUKV in the presence of competitors of high-mannose N-glycans or neutralizing antibodies (Abs), virus binding was abolished. L-SIGN arguably binds phleboviruses through direct interactions with N-glycans on the viral glycoproteins, as reported for most interactions between other viruses and C-type lectins.

In DC-SIGN-expressing cells, the lectin is distributed within clusters of different sizes (6,31). Similar to these observations, L-SIGN was found at the cell surface in lectin-containing membrane patches with heterogeneous sizes. In cells expressing DC-SIGN, UUKV has been shown
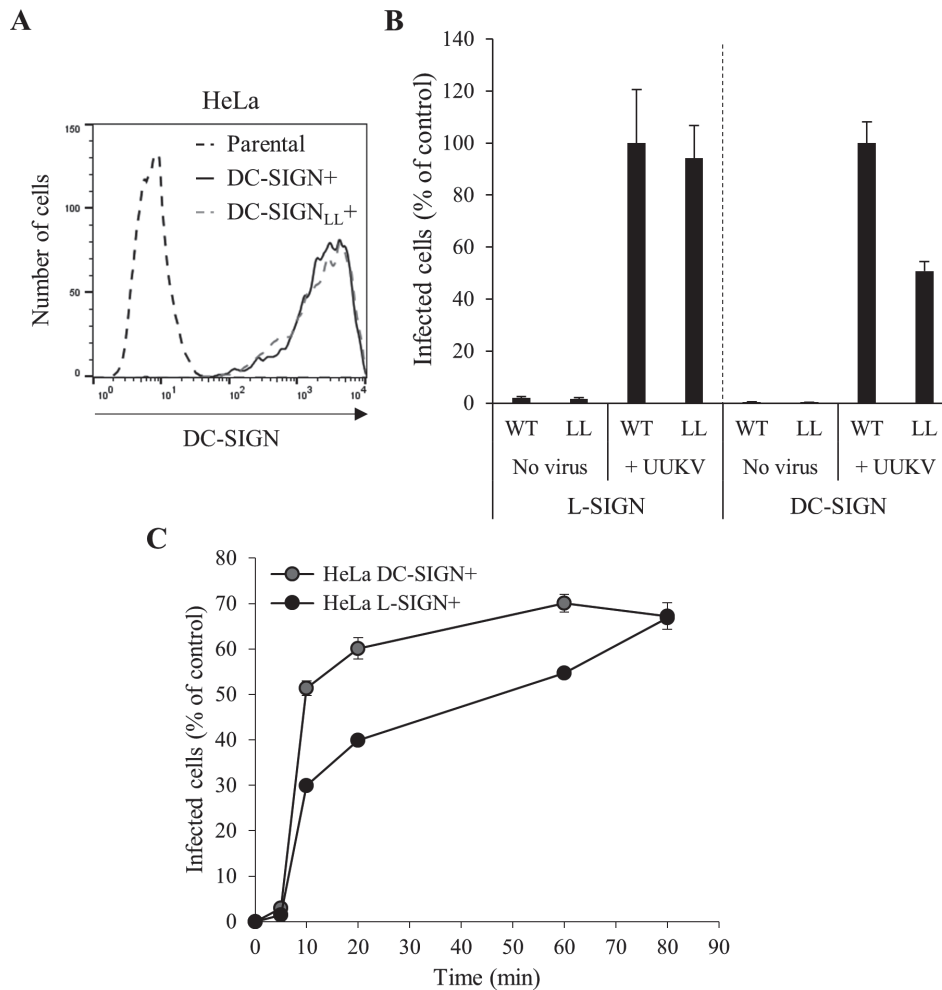
Figure 7: UUKV internalization and endosomal escape into DC-SIGN- and L-SIGN-expressing cells. A) Expression of DC-SIGN and its endocytosis-defective mutant was detected on HeLa cells (HeLa DC-SIGN+ or HeLa DC-SIGN$_{LL}$+ respectively) using flow cytometry after immunostaining with the Fab 1621P. B) HeLa cells that express L-SIGN, DC-SIGN, and the corresponding endocytosis-defective mutants (L-SIGN$_{LL}$ or DC-SIGN$_{LL}$, respectively) were assessed for UUKV replication 7 h post-infection (MOI ~1). Cells positive for the UUKV protein N were quantified using flow cytometry. Infection was normalized to the infected HeLa cells expressing the WT lectin (% of control). C) HeLa DC-SIGN+ and HeLa-L-SIGN+ cells were exposed to UUKV (MOI ~3) on ice, washed and rapidly warmed. NH$_4$Cl (50 mM) was added at different times to block further penetration. Infection was detected using flow cytometry 16 h later and normalized to infection in the absence of NH$_4$Cl.

to collect additional molecules of the receptor to the site of contact, thus generating a receptor-rich microdomain in the plasma membrane (PM) (6). Elucidating whether UUKV induces clustering of L-SIGN remains paramount. The lipid and protein composition and other properties may differ in these virus-induced membrane patches from the membrane at large, and consequently, significantly influence the subsequent signal transduction and endocytosis.

Using Abs, it has been shown that crosslinking on the cell surface is required to induce efficient endocytosis of DC-SIGN (31). DC-SIGN has also been recently reported to be involved in different signaling pathways (32,33). When Abs against the ectodomain of L-SIGN were used in binding, the lectin was dramatically redistributed into the cells. Hence, it is highly probable that Abs allow the clustering of L-SIGN and the activation of a signaling pathway that triggers the endocytic uptake of the receptor cluster.

Although relatively short, the cytoplasmic tail of DC-SIGN and L-SIGN carries several signaling and internalization motifs. DC-SIGN critically relies on its cytosolic LL motif for the endocytosis of cargo (34,35). When we expressed a mutant of L-SIGN lacking the LL motif in the cytosolic tail, Abs failed to trigger the internalization of the lectin. The LL-motif acts as a typical docking site for adaptor proteins required for the formation of clathrin-coated pits (CCPs), and therefore, receptor-induced clathrin-mediated endocytosis (CME) (24,36). It is reasonable to assume that L-SIGN sorts cargo into the endocytic machinery via CME.

Our results contrast with a previous report on DC-SIGN, for which it is proposed that the lectin is an entry receptor required for both virus attachment and endocytosis into DCs (6). When the endocytosis-defective mutant of L-SIGN was expressed, UUKV particles still attached to the cells. Viruses were internalized and there was infection. We cannot completely rule out that L-SIGN by itself mediates virus internalization, as deletion of the LL type endocytosis signal often makes endocytosis of receptors less efficient rather than preventing endocytosis. However, our findings suggest that UUKV entry can be dissociated from lectin internalization, and the most likely scenario is that L-SIGN acts as an attachment factor for phleboviruses.

Parental HeLa cells, but not Raji cells, showed minimal but significant levels of UUKV infection at higher MOIs. In addition, L-SIGN was more efficient to promote infection of HeLa cells than Raji cells. Together this suggests the presence of a broadly specific alternative receptor(s) with relatively low affinity. In this model, such a receptor molecule(s) would mediate phlebovirus attachment and entry with very poor efficiency in the absence of L-SIGN. Several lines of evidence implicate cellular receptors for phosphatidylserine in cell entry of emerging enveloped RNA viruses, in particular members of the TAM and TIM families (37–40). Because TAM receptors, in particular Axl, are expressed on many endothelial cells and in most HeLa cell lines, they may represent interesting co-receptor candidates to examine in the future.

The general properties and dynamics of UUKV entry were faster and more efficient in cells expressing DC-SIGN than L-SIGN. The incapacity of the DC-SIGN mutant to internalize the virus certainly modifies the global dynamics of

virus-lectin interactions at the cell surface. In such a situation, it is conceivable that the DC-SIGN mutant-dependent infection implicates a co-receptor, most likely the same than that involved in the L-SIGN-dependent UUKV internalization. However this pathway seems to promote infection in a less extend than the normal entry route implying the endocytic activity of DC-SIGN. Cells expressing the DC-SIGN endocytosis-defective mutant are significantly less sensitive to UUKV than those expressing the WT lectin. The dynamics of the virus internalization directly through the lectin arguably determines the global efficiency of the infectious entry process.

Once the UUKV particles reached endosomes, our results indicated that viruses accumulated in the perinuclear region 20 min after internalization. This is a typical location for LE vacuoles and is compatible with the late penetration of bunyaviruses (4,5). At this time, viruses remained associated with L-SIGN-containing endosomal vesicles. In DC-SIGN-expressing cells, UUKV particles separated from the lectin in early endosomes (EEs) within 5–10 min (6). DC-SIGN tetramers undergo acid-induced disassembly below pH 6.5–6.7, and thereby lose their high avidity for cargo in EEs (18,41). The effect of endosomal acidification on L-SIGN tetramers and release of cargo into endosomes remains unclear (18,42,43). We observed that UUKV particles remained associated within L-SIGN-positive vesicles 30 min after internalization. While we cannot exclude that viruses do not continue to interact with the lectin at this time, our results indicate that L-SIGN does not belong to the receptors that recycle from EEs to the PM, another major distinction with DC-SIGN (6).

Confirmation of these findings under physiological conditions remains challenging as primary human LSECs are extremely difficult to obtain due to scarcity of liver resections. However, we propose that by acting as an attachment receptor on LSECs, L-SIGN plays a role in the liver tropism of bunyaviruses. Beyond the importance of L-SIGN in bunyavirus infection, our results provide an indication of added complexity in the interactions between C-type lectins and viruses that are not simply limited to carbohydrate recognition. As for many other signaling virus receptors, the details of the transition processes between the extracellular and intracellular stages remain to

be addressed and represent a challenge for future research in the field (24). With regards to this, UUKV appears to be a precious tool to study the endocytic receptor function of C-type lectins and to improve our understanding of the dynamics of virus–receptor interactions in general.

Materials and Methods

Cells

All products used for cell culture were from Life Technologies. Human B cells (Raji) and human epithelial cells (HeLa) were maintained in RPMI and DMEM, respectively, supplemented with 10% serum and antibiotics (100 µg/mL streptomycin and 100 U/mL penicillin). HeLa cells that stably express L-SIGN (NCBI, NP_055072) or the mutant L-SIGN$_{LL}$ were obtained by transduction with the TRIPΔU3 lentiviral vector coding for the corresponding form of the lectin as previously reported for DC-SIGN and its endocytosis-defective mutant DC-SIGN$_{LL}$ (21,35). L-SIGN$_{LL}$ was generated by site-directed mutagenesis (LL/AA, QuikChange Lightning kit, Agilent) of the TRIPΔU3 lentiviral vector encoding L-SIGN WT. Different levels of lectin expression were obtained by fluorescent-activated cell sorting (FACS) following immunofluorescence staining against the lectin. Raji cells expressing L-SIGN as well as Raji and HeLa cells expressing DC-SIGN or its endocytosis-defective form DC-SIGN$_{LL}$ have been already described (6,21,35,44).

Viruses

RVFV recombinant ZH548 strain (rRVFV-ΔNSs-EGFP), which codes for the EGFP reporter gene in place of the virulent factor NSs, was rescued from plasmid DNAs and amplified in Vero cells (22). The prototype strains of TOSV ISS and UUKV S23 have been described previously (45–47). Production, purification and titration of TOSV and UUKV were performed in the mammalian Vero and BHK-21 cells, respectively, as shown elsewhere (5,48). Labeling of UUKV with AF568-succinimidyl esters (Life Technologies) was performed in HEPES (20 mM) as recently described with other similar dyes (5,6). Three molecules of the dye were conjugated to one molecule of UUKV glycoprotein. The MOI is given according to the titers determined on BHK-21 (UUKV) and Vero (TOSV and rRVFV) cells.

Antibodies and reagents

The anti-DC-SIGN/L-SIGN mouse mAb 1621 and the anti-DC-SIGN mouse mAb 162 as well as the phycoerythrin (PE)- and fluorescein isothiocyanate (FITC)-conjugated Fab 1621P (anti-DC-SIGN/L-SIGN) and Fab 162F (anti-L-SIGN) were all purchased from R&D Systems. The mouse mAb 8B11A3 targets a linear epitope in the UUKV protein N and is a kind gift from A.K. Överby and Ludwig Institute for Cancer Research (Stockholm, Sweden) (49). The rabbit polyclonal antibody (pAb) U2 is directed against all the UUKV structural proteins (6). The mouse immune ascitic fluid against all TOSV structural proteins is a generous gift from R.B. Tesh (University of Texas, Galveston, Texas, USA). NH$_4$Cl, mannan

and EGTA stocks were all from Sigma and dissolved in water. Bafilomycin A1 (Sigma) was dissolved in absolute methanol.

Flow cytometry-based detection of L-SIGN at the cell surface

Surface expression of L-SIGN was performed as previously reported (35). Briefly, cells expressing L-SIGN were harvested with PBS containing 1 mM EDTA to maintain all the surface proteins intact, and incubated with the PE-conjugated Fab 1621P (1:50) for 1 h on ice in PBS with 2% serum before analysis using flow cytometry.

Infection assays

Cells were exposed to viruses at 37°C in binding buffer (RPMI pH ~7.4 containing 0.2% BSA, 1 mM CaCl$_2$ and 2 mM MgCl$_2$) at indicating MOIs for 1 h. Virus supernatant was replaced by culture medium and samples incubated at 37°C for up to 48 h. For inhibition assays, cells were pretreated with inhibitors at the indicated concentrations for 30 min and exposed to UUKV in the continuous presence of the inhibitors. When the lectin expression was assayed concomitantly to the viral replication, cells were harvested with PBS containing 1 mM EDTA to maintain intact all the surface proteins. After fixation and permeabilization with 0.1% saponin, infected cells were incubated with primary Abs against viral proteins at room temperature (RT) for 1 h, washed, and subsequently exposed to AF-conjugated secondary Ab (1:500, Life Technologies) at RT for 45 min. The mAb 8B11A3 (1:400) and a mouse immune ascitic fluid (1:400) were used to detect intracellular UUKV and TOSV antigens, respectively. Cells infected with rRVFV-ΔNSs-EGFP were assayed following fixation for the EGFP signal. When the mAb 1621 (25 µg/mL) and Fab 1621P (1:50) were used in infection assay to neutralize or detect L-SIGN, respectively, UUKV-infected cells were stained with the pAbs U2 (1:400). The infection was monitored either using wide-field fluorescence microscopy or flow cytometry.

Virus binding and internalization

Viruses were bound to the cells on ice in binding buffer for 1 h at the indicated MOIs or concentrations of UUKV glycoproteins (6,50). Cells were maintained in the cold or rapidly warmed to 37°C for 30 min. Binding was analyzed using flow cytometry or fluorescence confocal microscopy. For binding inhibition, cells were pretreated with inhibitors at the indicated concentrations for 30 min and then exposed to viruses in the presence of the inhibitors. Internalization of the viruses was monitored in fixed or live samples using confocal microscopy. When co-localization of the viruses with L-SIGN was assessed, virus-bound cells were immunostained with the mAb 1621 or mAb 162 (1 µg/mL) and then an AF488-coupled secondary mAb (1:1,000, Life Technologies) before imaging.

Internalization of L-SIGN

Internalization of L-SIGN was monitored as previously described for DC-SIGN (35). Briefly, HeLa cells expressing L-SIGN or L-SIGN$_{LL}$ were seeded on coverslips. The following day, cells were incubated with the anti-L-SIGN Fab 162F (1 µg/mL) in PBS with 2% serum in the cold for

1 h. Cells were then washed to remove unbound Ab and rapidly shifted to 37°C for up to 30 min to allow Ab-induced L-SIGN endocytosis. Cells were fixed and analyzed using confocal microscopy.

NH₄Cl add-in time course

NH$_4$Cl add-in time course and PM-virus fusion assays were performed as recently reported (5). Briefly, virus binding (MOI ∼ 3) was synchronized on ice. Virus-bound cells were rapidly warmed to 37°C, and NH$_4$Cl (50 mM) was added at the indicated times (up to 80 min). Cells were subsequently incubated at 37°C and harvested 7 h later.

Flow cytometry and fluorescence microscopy

Flow cytometry-based analysis involved the use of a FACS Calibur cytometer (Becton Dickinson) and Flowjo software (Treestar). For wide-field microscopy, nuclei were stained with Hoechst 33258 (1 µg/mL, Life Technologies) and cells imaged with an Olympus IX81 microscope. Confocal microscopy in fixed samples was performed with either a Zeiss LSM700 microscope or a Leica TCS SP2 microscope whilst live cells were imaged with a Nikon TiE Eclipse microscope equipped with a PerkinElmer UltraVIEW VoX 3D module.

Statistical analysis

The data shown are representative of at least three independent experiments. Values are given as the mean of triplicates ± standard deviation (SD).

Acknowledgments

Supporting Information

Additional Supporting Information may be found in the online version of this article:

Movie S1. UUKV uptake into L-SIGN-expressing cells. This movie is related to Figures 3A and 7C. UUKV-AF568 (MOI ∼ 3) was added to L-SIGN-expressing HeLa cells. Cells were visualized using spinning-disc confocal microscopy at 37°C in the continuous presence of the virus. Images were taken at 1/53 Hz in one focal plane for 60 min. The video is displayed at 10 Hz. Virus particles (red) are seen being internalized rapidly into cells (differential interference contrast).

Movie S2. UUKV uptake into DC-SIGN-expressing cells. This movie is related to Figure 7C. Live imaging of UUKV-AF568 uptake into DC-SIGN-expressing HeLa cells was performed, monitored and analyzed following the same procedure as that for Movie S1, Supporting Information.

References

1. Leger P, Lozach PY. Bunyaviruses: from transmission by arthropods to virus entry into the mammalian host first-target cells. Future Virol 2015;10:859–881.
2. Freiberg AN, Sherman MB, Morais MC, Holbrook MR, Watowich SJ. Three-dimensional organization of Rift Valley fever virus revealed by cryoelectron tomography. J Virol 2008;82:10341–10348.
3. Overby AK, Pettersson RF, Grunewald K, Huiskonen JT. Insights into bunyavirus architecture from electron cryotomography of Uukuniemi virus. Proc Natl Acad Sci USA 2008;105:2375–2379.
4. Lozach PY, Huotari J, Helenius A. Late-penetrating viruses. Curr Opin Virol 2011;1:35–43.
5. Lozach PY, Mancini R, Bitto D, Meier R, Oestereich L, Overby AK, Pettersson RF, Helenius A. Entry of bunyaviruses into mammalian cells. Cell Host Microbe 2010;7:488–499.
6. Lozach PY, Kuhbacher A, Meier R, Mancini R, Bitto D, Bouloy M, Helenius A. DC-SIGN as a receptor for phleboviruses. Cell Host Microbe 2011;10:75–88.
7. Nfon CK, Marszal P, Zhang S, Weingartl HM. Innate immune response to Rift Valley fever virus in goats. PLoS Negl Trop Dis 2012;6:e1623.
8. Peyrefitte CN, Perret M, Garcia S, Rodrigues R, Bagnaud A, Lacote S, Crance JM, Vernet G, Garin D, Bouloy M, Paranhos-Baccala G. Differential activation profiles of Crimean-Congo hemorrhagic fever virus- and Dugbe virus-infected antigen-presenting cells. J Gen Virol 2010;91:189–198.
9. Connolly-Andersen AM, Douagi I, Kraus AA, Mirazimi A. Crimean-Congo hemorrhagic fever virus infects human monocyte-derived dendritic cells. Virology 2009;390:157–162.
10. McElroy AK, Nichol ST. Rift Valley fever virus inhibits a pro-inflammatory response in experimentally infected human monocyte derived macrophages and a pro-inflammatory cytokine response may be associated with patient survival during natural infection. Virology 2012;422:6–12.
11. Hofmann H, Li X, Zhang X, Liu W, Kuhl A, Kaup F, Soldan SS, Gonzalez-Scarano F, Weber F, He Y, Pohlmann S. Severe fever with thrombocytopenia virus glycoproteins are targeted by neutralizing antibodies and can use DC-SIGN as a receptor for pH-dependent entry into human and animal cell lines. J Virol 2013;87:4384–4394.
12. Gommet C, Billecocq A, Jouvion G, Hasan M, Zaverucha do Valle T, Guillemot L, Blanchet C, van Rooijen N, Montagutelli X, Bouloy M, Panthier JJ. Tissue tropism and target cells of NSs-deleted rift valley fever virus in live immunodeficient mice. PLoS Negl Trop Dis 2011;5:e1421.

13. Madani TA, Al-Mazrou YY, Al-Jeffri MH, Mishkhas AA, Al-Rabeah AM, Turkistani AM, Al-Sayed MO, Abodahish AA, Khan AS, Ksiazek TG, Shobokshi O. Rift Valley fever epidemic in Saudi Arabia: epidemiological, clinical, and laboratory characteristics. Clin Infect Dis 2003;37:1084–1092.

14. Burt FJ, Swanepoel R, Shieh WJ, Smith JF, Leman PA, Greer PW, Coffield LM, Rollin PE, Ksiazek TG, Peters CJ, Zaki SR. Immunohistochemical and in situ localization of Crimean-Congo hemorrhagic fever (CCHF) virus in human tissues and implications for CCHF pathogenesis. Arch Pathol Lab Med 1997;121:839–846.

15. Le Coupanec A, Babin D, Fiette L, Jouvion G, Ave P, Misse D, Bouloy M, Choumet V. Aedes mosquito saliva modulates Rift Valley fever virus pathogenicity. PLoS Negl Trop Dis 2013;7:e2237.

16. Chen XP, Cong ML, Li MH, Kang YJ, Feng YM, Plyusnin A, Xu J, Zhang YZ. Infection and pathogenesis of Huaiyangshan virus (a novel tick-borne bunyavirus) in laboratory rodents. J Gen Virol 2012;93: 1288–1293.

17. Pustylnikov S, Sagar D, Jain P, Khan ZK. Targeting the C-type lectins-mediated host-pathogen interactions with dextran. J Pharm Pharm Sci 2014;17:371–392.

18. Guo Y, Feinberg H, Conroy E, Mitchell DA, Alvarez R, Blixt O, Taylor ME, Weis WI, Drickamer K. Structural basis for distinct ligand-binding and targeting properties of the receptors DC-SIGN and DC-SIGNR. Nat Struct Mol Biol 2004;11:591–598.

19. Mitchell DA, Fadden AJ, Drickamer K. A novel mechanism of carbohydrate recognition by the C-type lectins DC-SIGN and DC-SIGNR. Subunit organization and binding to multivalent ligands. J Biol Chem 2001;276:28939–28945.

20. Goncalves AR, Moraz ML, Pasquato A, Helenius A, Lozach PY, Kunz S. Role of DC-SIGN in Lassa virus entry into human dendritic cells. J Virol 2013;87:11504–11515.

21. Lozach PY, Amara A, Bartosch B, Virelizier JL, Arenzana-Seisdedos F, Cosset FL, Altmeyer R. C-type lectins L-SIGN and DC-SIGN capture and transmit infectious hepatitis C virus pseudotype particles. J Biol Chem 2004;279:32035–32045.

22. Billecocq A, Gauliard N, Le May N, Elliott RM, Flick R, Bouloy M. RNA polymerase I-mediated expression of viral RNA for the rescue of infectious virulent and avirulent Rift Valley fever viruses. Virology 2008;378:377–384.

23. Lozach PY, Lortat-Jacob H, de Lacroix de Lavalette A, Staropoli I, Foung S, Amara A, Houles C, Fieschi F, Schwartz O, Virelizier JL, Arenzana-Seisdedos F, Altmeyer R. DC-SIGN and L-SIGN are high affinity binding receptors for hepatitis C virus glycoprotein E2. J Biol Chem 2003;278:20358–20366.

24. Boulant S, Stanifer M, Lozach PY. Dynamics of virus-receptor interactions in virus binding, signaling, and endocytosis. Viruses 2015;7:2794–2815.

25. Dakappagari N, Maruyama T, Renshaw M, Tacken P, Figdor C, Torensma R, Wild MA, Wu D, Bowdish K, Kretz-Rommel A. Internalizing antibodies to the C-type lectins, L-SIGN and DC-SIGN, inhibit viral glycoprotein binding and deliver antigen to human dendritic cells for the induction of T cell responses. J Immunol 2006;176:426–440.

26. Van Breedam W, Pohlmann S, Favoreel HW, de Groot RJ, Nauwynck HJ. Bitter-sweet symphony: glycan-lectin interactions in virus biology. FEMS Microbiol Rev 2014;38:598–632.

27. Pokidysheva E, Zhang Y, Battisti AJ, Bator-Kelly CM, Chipman PR, Xiao C, Gregorio GG, Hendrickson WA, Kuhn RJ, Rossmann MG. Cryo-EM reconstruction of dengue virus in complex with the carbohydrate recognition domain of DC-SIGN. Cell 2006;124:485–493.

28. Bertolotti-Ciarlet A, Smith J, Strecker K, Paragas J, Altamura LA, McFalls JM, Frias-Staheli N, Garcia-Sastre A, Schmaljohn CS, Doms RW. Cellular localization and antigenic characterization of crimean-congo hemorrhagic fever virus glycoproteins. J Virol 2005;79: 6152–6161.

29. Antic D, Wright KE, Kang CY. Maturation of Hantaan virus glycoproteins G1 and G2. Virology 1992;189:324–328.

30. Sanchez AJ, Vincent MJ, Nichol ST. Characterization of the glycoproteins of Crimean-Congo hemorrhagic fever virus. J Virol 2002;76:7263–7275.

31. Neumann AK, Thompson NL, Jacobson K. Distribution and lateral mobility of DC-SIGN on immature dendritic cells − implications for pathogen uptake. J Cell Sci 2008;121:634–643.

32. Gringhuis SI, den Dunnen J, Litjens M, van der Vlist M, Geijtenbeek TB. Carbohydrate-specific signaling through the DC-SIGN signalosome tailors immunity to *Mycobacterium tuberculosis*, HIV-1 and *Helicobacter pylori*. Nat Immunol 2009;10:1081–1088.

33. Gringhuis SI, den Dunnen J, Litjens M, van Het Hof B, van Kooyk Y, Geijtenbeek TB. C-type lectin DC-SIGN modulates Toll-like receptor signaling via Raf-1 kinase-dependent acetylation of transcription factor NF-kappaB. Immunity 2007;26:605–616.

34. Sol-Foulon N, Moris A, Nobile C, Boccaccio C, Engering A, Abastado JP, Heard JM, van Kooyk Y, Schwartz O. HIV-1 Nef-induced upregulation of DC-SIGN in dendritic cells promotes lymphocyte clustering and viral spread. Immunity 2002;16:145–155.

35. Lozach PY, Burleigh L, Staropoli I, Navarro-Sanchez E, Harriague J, Virelizier JL, Rey FA, Despres P, Arenzana-Seisdedos F, Amara A. Dendritic cell-specific intercellular adhesion molecule 3-grabbing non-integrin (DC-SIGN)-mediated enhancement of dengue virus infection is independent of DC-SIGN internalization signals. J Biol Chem 2005;280:23698–23708.

36. Braulke T, Bonifacino JS. Sorting of lysosomal proteins. Biochim Biophys Acta 2009;1793:605–614.

37. Morizono K, Chen IS. Role of phosphatidylserine receptors in enveloped virus infection. J Virol 2014;88:4275–4290.

38. Morizono K, Xie Y, Olafsen T, Lee B, Dasgupta A, Wu AM, Chen IS. The soluble serum protein Gas6 bridges virion envelope phosphatidylserine to the TAM receptor tyrosine kinase Axl to mediate viral entry. Cell Host Microbe 2011;9:286–298.

39. Meertens L, Carnec X, Lecoin MP, Ramdasi R, Guivel-Benhassine F, Lew E, Lemke G, Schwartz O, Amara A. The TIM and TAM families of phosphatidylserine receptors mediate dengue virus entry. Cell Host Microbe 2012;12:544–557.

40. Jemielity S, Wang JJ, Chan YK, Ahmed AA, Li W, Monahan S, Bu X, Farzan M, Freeman GJ, Umetsu DT, Dekruyff RH, Choe H. TIM-family proteins promote infection of multiple enveloped viruses through

virion-associated phosphatidylserine. PLoS Pathog 2013;9: e1003232.

41. Tabarani G, Thepaut M, Stroebel D, Ebel C, Vives C, Vachette P, Durand D, Fieschi F. DC-SIGN neck domain is a pH-sensor controlling oligomerization: SAXS and hydrodynamic studies of extracellular domain. J Biol Chem 2009;284:21229–21240.

42. Gramberg T, Soilleux E, Fisch T, Lalor PF, Hofmann H, Wheeldon S, Cotterill A, Wegele A, Winkler T, Adams DH, Pohlmann S. Interactions of LSECtin and DC-SIGN/DC-SIGNR with viral ligands: differential pH dependence, internalization and virion binding. Virology 2008;373: 189–201.

43. Probert F, Mitchell DA, Dixon AM. NMR evidence for oligosaccharide release from the dendritic-cell specific intercellular adhesion molecule 3-grabbing non-integrin-related (CLEC4M) carbohydrate recognition domain at low pH. FEBS J 2014;281:3739–3750.

44. Burleigh L, Lozach PY, Schiffer C, Staropoli I, Pezo V, Porrot F, Canque B, Virelizier JL, Arenzana-Seisdedos F, Amara A. Infection of dendritic cells (DCs), not DC-SIGN-mediated internalization of human immunodeficiency virus, is required for long-term transfer of virus to T cells. J Virol 2006;80:2949–2957.

45. Giorgi C, Accardi L, Nicoletti L, Gro MC, Takehara K, Hilditch C, Morikawa S, Bishop DH. Sequences and coding strategies of the S RNAs of Toscana and Rift Valley fever viruses compared to those of Punta Toro, Sicilian Sandfly fever, and Uukuniemi viruses. Virology 1991;180:738–753.

46. Laughlin LW, Meegan JM, Strausbaugh LJ, Morens DM, Watten RH. Epidemic Rift Valley fever in Egypt: observations of the spectrum of human illness. Trans R Soc Trop Med Hyg 1979;73:630–633.

47. Pettersson R, Kaariainen L. The ribonucleic acids of Uukuniemi virus, a noncubical tick-borne arbovirus. Virology 1973;56:608–619.

48. Billecocq A, Vialat P, Bouloy M. Persistent infection of mammalian cells by Rift Valley fever virus. J Gen Virol 1996;77:3053–3062.

49. Persson R, Pettersson RF. Formation and intracellular transport of a heterodimeric viral spike protein complex. J Cell Biol 1991;112:257–266.

50. Meier R, Franceschini A, Horvath P, Tetard M, Mancini R, von Mering C, Helenius A, Lozach PY. Genome-wide small interfering RNA screens reveal VAMP3 as a novel host factor required for Uukuniemi virus late penetration. J Virol 2014;88:8565–8578.